Transport in Porous Media **17:** 285–303, 1994.

Modelling the Capillary Imbibition Kinetics in Sedimentary Rocks: Role of Petrographical Features

CLAUDE HAMMECKER and DANIEL JEANNETTE
Centre de Géochimie de la Surface (CNRS), 67084 Strasbourg Cedex, France

(Received: 7 December 1993; in final form, 24 August 1994)

Abstract. The kinetics of capillary imbibition into sedimentary rocks has been measured experimentally and calculated with a model that has been described previously by Hammecker and colleagues (1993). The validity of this model has been discussed and compared to other models. Three limestones, two clean sandstones and three clayey sandstones have been studied. The capillary processes are discussed as a function of their petrography and the pore structures. The role of the grain surface, described by the specific surface area, has been especially studied. The influence of clay coating on detrital grains on capillary processes has been quantified.

Key words: Capillary imbibition kinetics, sandstone, limestone, pore radii, specific surface area, clay content, coating.

Nomenclature

- A weight increase rate by capillary imbibition ($A = \Delta W/(S_1\sqrt{t})$)
- B capillary rise rate ($B = \Delta l/\sqrt{t}$)
- l height of the capillary fringe or the meniscus over the free water level
- g gravitational constant
- L height of the geometrical elements
- P_a pressure in the air
- P_c capillary pressure
- P_w pressure in the water
- Q flow rate
- N_f free porosity
- N_t total porosity
- r radius of the pore (meniscus)
- r_1 pore access radius (neck)
- R pore radius (widening)
- R_s particle radius

S specific surface area
S_I macroscopical area of the sample surface throughout which imbibition occurs
t time
W weight
z height
γ surface tension
η dynamic viscosity
θ contact angle
ρ density
ρ_r true density

0. Introduction

The study of capillary imbibition kinematics of water in rocks is motivated by the fact that it is one of the most important physical parameters governing the water transfer in unsaturated conditions. These water transfer mechanisms govern many geological processes, e.g. the alteration of rocks in superficial conditions, and especially the decay processes in monumental stones (Lewin and Charola, 1979; Amoroso, 1983; Jeannette and Hammecker, 1992; Hammecker, 1993).

The capillary imbibition kinematics of water into sedimentary rocks can be measured experimentally, and two basic parameters can be defined: the rate of capillary rise and the amount of absorbed water. Their values are indicative of the porous network geometry and of the mineralogical composition of the rocks.

The imbibition kinetics of water in porous media is described by many theoretical tube models, mainly based on the Washburn (1921) law. They describe the imbibition phenomenon in geometrical shaped pores (Szekely *et al.*, 1971; Dullien, 1979; Levine *et al.*, 1980), which closely resemble the imbibition process observed in rocks. However, in order to find the right imbibition kinetics, the dimensions of pores introduced into these models do not usually agree with experimental data. With the model proposed by Hammecker *et al.* (1993), based on a tube model composed of a stack of hollow spherical elements, the real pore dimensions (microscopic observation, mercury porosimetry and BET surface area) are introduced in the calculus in order to obtain simulated imbibition kinetic values which agree with the experimental ones.

Based on this theoretical tube model which describes the capillary imbibition kinetics of porous networks, the experimental and calculated values for different kinds of sedimentary rocks have been compared and related to the petrographical features.

1. Petrography

This study has been performed with eight different types of sedimentary rocks in order to check the validity of this model: three limestones (Laspra, Hontoria, Lourdines), two clean sandstones (Fontainebleau, Gueberschwihr) and three clayey sandstones (Darney, Rosheim, Osenbach). These rocks have been chosen for their petrographical differences and for their frequent use on buildings in Spain and in France.

Laspra limestone is a fine dolomicritic lacustrine deposit of an Eocene basin, situated in the central part of Asturias (NW Spain). It is constituted of a very fine micritic matrix with characea, micritical intraclasts and some detrital quartz grains of 50 to 100 μm. Despite some local pores formed by dissolution, the very high porosity of this rock ($N_t = 30\%$) is mainly due to the microporous medium formed by the micritic matrix, which represents a freely interconnected framework. On the other hand, the macropores usually represent a part of the pore volume that is not involved in the capillary imbibition because of the presence of air bubbles trapped in these areas (trapped porosity).

Lourdines limestone is a Callovian calcareous micrit of the northern margin of the Aquitanian Basin, exposed along the Clain valley in the area of Poitiers (W France). This limestone is formed by microporous intraclasts of 50 to 150 μm diameter, and some shell debris, sealed in a sparitic cement. As the packing of the intraclasts is quite dense, the sparitic cement is not very abundant. The total porosity of 23% is mainly due to the microporous intraclasts. However, some intergranular macropores (5 to 15 μm), forming the trapped porosity, can be observed.

Hontoria limestone is a turonian bioclastic limestone from Spanish meseta in the area of Burgos (prov. Castilla -León, Spain), composed of centimetrical debris of lamellibranch shells, bryozoaires, crinoid remains, and oolithic intraclasts sealed with a sparitic cement. The cement is formed by the coalescence of calcite crystals growing on the surface of the clasts. The porosity of this rock ($N_t = 19.8\%$) is formed by an important intraclastic microporosity but especially by intergranular macropores (100 μm), the surfaces of which are covered by well-formed calcite micro-crystallites of 10 to 15 μm diameter.

In the basin of Paris the *Fontainebleau sandstone* is formed by Stampian (Middle Oligocene) eolian sand, locally hardened by silicification due to variations of the water table. The samples used in this study are from the area of Milly-la Forêt. This sandstone is extremely pure, because it is formed by a packing of quartz grains of about 300 μm. An important characteristic of this sandstone is the high silicification to which it has been submitted, illustrated by polyhedral quartz overgrowth. The wide initial pore space is partially sealed by the geometrical silicifications so that the total porosity (N_t) does not exceed 11%. The free porosity, corresponding to the pore volume which is freely invaded by water under atmospheric capillary imbibition conditions (air bubbles remain in 'trapped

porosity'), represents less than 5%. The free porosity is formed by thin and long voids, remaining between the quartz overgrowth, and by large pores covered small quartz crystals.

Gueberschwihr sandstone is a feldspatic sandstone of the Middle Buntsandstein ('Grès Vosgiens'), from the western margin of the Rhine graben (Alsace, NE of France). In the area of Gueberschwihr, near a main sub-meridian fault system, most of this sandstone is highly silicified. The detrital grains of quartz, K-feldspar and lithic elements have rounded shapes and initial diameters of 400 to 750 μm. The concavo-convex contacts between the detrital grains are indicative of diagenetic conditions related to the 1000 m burial, which the Buntsandstein layers reached in NE of France during the Oligocene. Later hydrothermal modifications, especially the important silicifications, sealed the intergranular pore space by developing quartz and sometimes feldspar overgrowth with euhedral crystalline faces. Silicification is so advanced that no voids between the different quartz overgrowth can be observed. As a consequence the total porosity of this sandstone, represented by geometrical intergranular voids and intragranular micropores in the centres of altered feldspars, is extremely low ($N_t = 6\%$).

Darney sandstone is a Triassic sandstone (intermediate sandstone layers of the Upper Buntsandstein) outcropping on the western side of the Vosges. This sandstone, showing an alternate bedding of different colours underlined by long muscovite laminae, is quite fine-grained and poorly compacted. The quartz, feldspar grains and lithic elements are massive and angular, and show tangential contacts between them, which attest to low burial conditions and poor diagenetic transformations. Consequently the grains have a loose packing, and the intergranular voids are very important, with sizes comparable to those of the grains. The result is a quite substantial total porosity for this rock ($N_t = 23.6\%$). As the detrital grains are coated with well crystallised illite, these intergranular macropores are rimed by a superficial microporous network, improving the capillary interconnections conditions between the bigger pores.

Rosheim sandstone is a very fine Triassic sandstone with an argillaceous matrix, belonging to the Upper Buntsandstein ('grès à Meules'). In the area of Rosheim, located on the western margin of the Rhine graben, this yellowish rock was subjected to light silicification. It is mainly formed by quartz grains which are associated with microlithic grains, with altered K-feldspar (6 to 8%), with kaolinite and with muscovite laminae. When the quartz and feldspar grains are not covered with a phyllitic coating, they are affected by light silicifications due to pressure-solution phenomena. By the imbrication of several grains, polycrystalline areas are formed, which enclose clayey clusters and delineate tiny pores. The arrangement of these polycrystalline area determines the sandstones structure, and, in particular, the porous network. Depending on their arrangement, they form intergranular macropores whether they are occupied or rimed by clays, and this determines a total porosity (N_t) of 18.3%.

Osenbach sandstone is also a clayey sandstone of the Upper Buntsandstein ('Grès a Meules') outcropping in the occidental margin of the Rhine graben in Alsace (NE of France). This rock is very fine-grained, with stratification planes delimited by mica concentrations and it is formed by elongated quartz and feldspar grains of 50 to 80 μm long and 30 to 40 μm wide. Corroded calcite crystals seal the intergranular pore space between the angular detrital grains, dropping the total porosity to 11.6%. When the quartz and feldspar grains are touching, they are imbricated and form polycrystalline associations, which control the texture of the rock. Between these polycrystalline elements, some macropores of 40 to 80 μm can be observed whereas usually they are occupied by illite clusters coloured by iron oxy-hydroxide concentrations.

2. Capillary Imbibition Kinetics Experiment

When rocks are exposed at the surface, for example, when they are used on buildings, their porous networks are never completely saturated with water. In these unsaturated conditions, menisci between water and air are formed in the pores. Consequently capillary pressure must be taken into account in the water transfer pressure gradients. The quantification of the water balance is an important datum for the control of decay processes in rocks on monuments. Hence, is it necessary to quantify the capillary imbibition kinetics which are usually measured experimentally on rock samples.

The imbibition experiments are generally performed with cylindrical rock samples having a diameter of 3.5 or 4 cm and a height of about 7 cm. They are previously oven dried at 60°C to reach wieght stabilisation, and they are then cooled at 20°C in a closed container in the presence of silica gel, in order to maintain a dry atmosphere. Afterwards they are placed vertically on thick, wet filter paper which provides a continuous water supply. In order to prevent evaporation during the measurements, the samples are enclosed in an air-tight container to maintain a vapour saturated atmosphere. At increasing time intervals, the samples are weighed and the height of the wetted fringe observable on the surface of these samples is measured. Both the weight increase per unit surface ($\Delta W/S_1$), and the rise of the capillary fringe (Δl) are then plotted versus the square root of time ($\sqrt{t}$) (Figure 1). With this kind of representation, the capillary imbibition kinetics show a linear evolution, which can be easily quantified, by calculating the slopes of the two straight lines. Two kinetic parameters are defined.

$$A = \Delta W/(S_1\sqrt{t}) \quad \text{and} \quad B = \Delta l/(\sqrt{t}).$$

Usually, when the porous networks of the considered rocks are homogeneous, these two parameters are related via the value of free-porosity (N_l), because each weight increase corresponds to a certain height of capillary rise: $N_l \approx A/B$. As this relation is verified for the studied rocks, only the capillary rise kinetic coefficient B will be considered further. Obviously, the evolution as a function of square

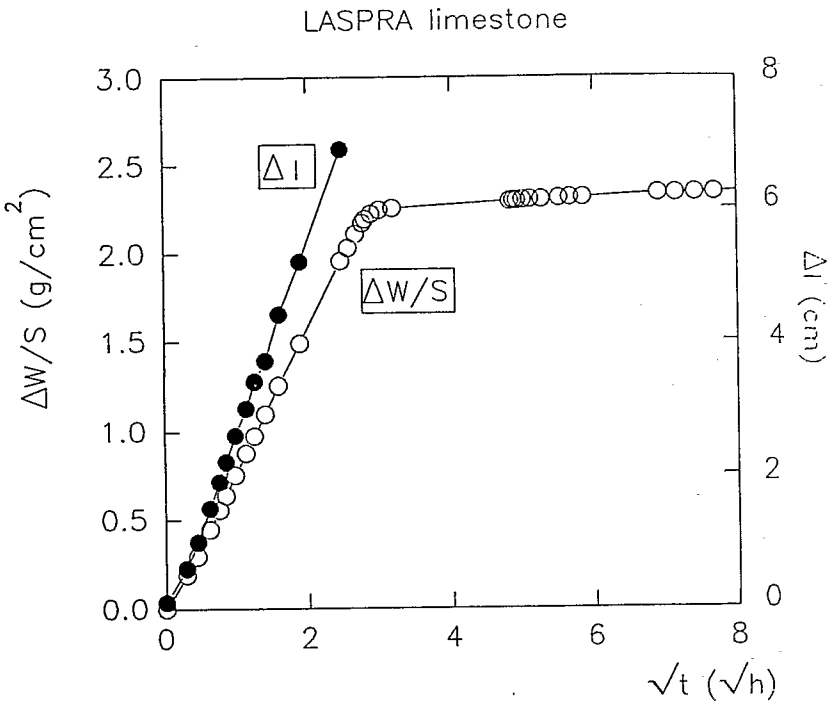

Fig. 1. Experimental capillary imbibition curve versus the square root of time. Hollow circles: weight increase per surface unit. Filled circles: height of the capillary fringe.

root of time is observed only as long as the influence of gravity can be neglected. Nevertheless the height of the cores and the pore sizes of the studied samples coincide with this simplification. The capillary imbibition parameters measured for these rocks show important differences ranging from $B = 0.6\,\text{cm h}^{-0.5}$ for Gueberschwihr sandstone to $B = 10.3\,\text{cm h}^{-0.5}$ for Fontainebleau sandstone, regardless of the porosity or the mineralogy.

3. Basic Principles of Water Transfer by Capillarity

The presence of the couple air-water in a porous medium is characterised by the presence of menisci indicative of a difference in pressure between the two phases. This difference, called capillary pressure (P_c), can be related to the radii of the menisci (r_1 and r_2) by the Laplace equation

$$P_c = P_a - P_w = \gamma\left(\frac{1}{r_1} + \frac{1}{r_2}\right), \tag{1}$$

where γ is surface tension of water ($0.072\,\text{Nm}^{-1}$). In a cylindrical tube, for example, when the meniscus is hemispherical, the capillary pressure is

$$P_c = \frac{2\gamma}{r}\cos\theta \tag{2}$$

with θ the contact angle of water on the solid surface in presence of air (generally $\theta = 0°$ for water on mineral surface).

The capillary pressure is one of the forces causing water transfer in porous media. However, the fluid transfer in a cylindrical tube, for example, is governed by the Hagen–Poiseuille law, where the fluid flow rate Q can be expressed as a function of fluid viscosity ($\eta = 1.019 \times 10^{-3} PI$), pressure gradient ($\Delta P$) and tube dimension (radius r and length l)

$$Q = \frac{r^4 \pi \Delta l'}{8\eta l}. \tag{3}$$

In the case of horizontal capillary imbibition, because gravity is neglected, the pressure gradient is the capillary pressure. Combining (2) and (3), Washburn (1921) related capillary imbibition kinetics to fluid properties and capillary dimension

$$l = \sqrt{\frac{r\gamma}{2\eta}t + l_0^2}. \tag{4}$$

When the initial height of the meniscus over the free water surface (l_0) is 0 at the beginning of the experiment ($t = 0$), the capillary rise and the weight increase can be formulated like simple square root functions

$$\begin{cases} l = B\sqrt{t} \\ v = A\sqrt{t} \end{cases} \text{ with } \begin{cases} B = \sqrt{r\gamma/2\eta} \\ A = \rho \cdot \pi \cdot r^2 \sqrt{r\gamma/2\eta}. \end{cases}$$

The Washburn equation shows a similar evolution for capillary imbibition kinetics as those measured experimentally (see Table I). Nevertheless, when the experimental values of pore radii are introduced directly to the Washburn cylinder model, the calculated and measured values of A and B show several orders of magnitude difference, even when gravity is considered (Mertz, 1991). Hence the simple cylindrical model is not really appropriate to quantify the capillary imbibition kinetics into the porous network of the sedimentary rock.

4. The Model

To describe mathematically the complex geometry of the porous network of rocks, it is necessary to introduce some very important simplifications. Most of the capillary imbibition or capillary pressure models involve simple pore shapes being defined as cylindrical, conical, sinusoidal or spherical (Kusakov and Nekrasov, 1966; Van

TABLE I. Experimental values of total porosity (N_t), free porosity (N_f), rate of weight increase (A), rate of capillary fringe migration (B)

Rock type	N_t(%)	N_f(%)	A(g cm^{-2} h$^{-0.5}$)	B(cm h$^{-0.5}$)
Laspra	30.03	28	0.64	2.39
Lourdines	25.8	22.8	1.04	5.5
Hontoria	19.83	18	0.94	7.1
Fontainebleau	10.8	4.8	0.38	10.3
Gueberschwihr	6.44	3.31	0.03	0.6
Darney	23.63	15.02	0.34	2.42
Rosheim	18.28	12.35	0.13	1.25
Osenbach	11.62	8.29	0.08	1.09

Barkel, 1975; Dullien *et al.*, 1977; Levine *et al.*, 1980; Marmur, 1989). Based on these kind of studies, a model of a tube composed of a stack of spherical elements has been devised (Hammecker *et al.*, 1993). Despite the poor resemblance of this model to a real, natural, porous network, it takes into account some important geometrical parameters, like the difference between the pore access radii and the proper pore radii. In order to check the importance of the actual geometry of the pore, three other shapes of revolution with radius variation along the axis of the capillary, have been tested in this paper: conical, sinusoidal, elliptical. Moreover the influence of the presence of a restriction, having a radius r_1, on a cylindrical tube with a radius R, has also been examined. Considering a vertical imbibition of such elements, the variation of the radius of the elements versus the height z can be written as

$$r(z) = \sqrt{(2Rz - z^2)}, \qquad \text{spherical},$$

$$r(z) = z\frac{R}{L}, \quad z < L \qquad \text{conical},$$

$$r(z) = R - \left((z-L)\frac{r}{L}\right), \quad z > L \qquad \text{conical},$$

$$r(z) = \left(\frac{R-r_1}{2}\right)\left(1 + \sin\left(\frac{2z\pi}{L}\right)\right) + r_1, \qquad \text{sinusoidal},$$

$$r(z) = \left(\frac{R-r_1}{2}\right)\left|\sin\left(\frac{z\pi}{L}\right)\right| + r_1, \qquad \text{elliptical},$$

$$r(z) = R, \qquad \text{cylindrical}.$$

where r_1 is the access radius to the hollow element, R is the maximum radius of the element and L is the height of the element (Figure 2). Assuming that the radius $r(z)$ of these theoretical pore shapes can be considered equivalent to the radius

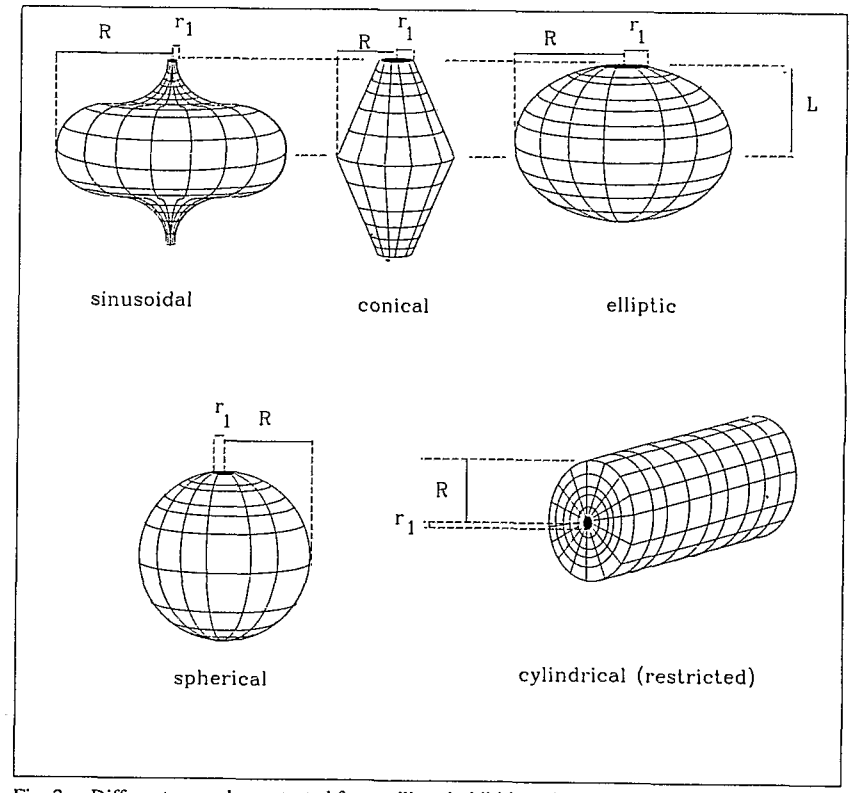

Fig. 2. Different pore shapes tested for capillary imbibition kinetics. R: maximum radius of the element; r_1: radius of the access to element, L: height of the element.

of the meniscus, the capillary pressure is a function of the height of the meniscus in the elements: $P_c(z) = \frac{2\gamma}{r(z)}$. The gravity acting as an adverse force to capillary rise, also depends on the height z of the meniscus and must be considered in the pressure gradient ΔP

$$\Delta P = \frac{2\gamma}{r(z)} - \rho g z, \tag{5}$$

where ρ is water density and g is the gravitational constant.

Based on the Hagen–Poiseuille law, the flow rate expression for capillary imbibition can be formulated

$$Q = \frac{r_1^4\pi}{8\eta z}\left(\frac{2\gamma}{r(z)} - \rho g z\right) = \frac{r(z)^2\pi\,\mathrm{d}z}{\mathrm{d}t}, \tag{6}$$

and after numerical integration of this expression the imbibition kinetics of the previously presented hollow elements can be calculated. Depending on the height

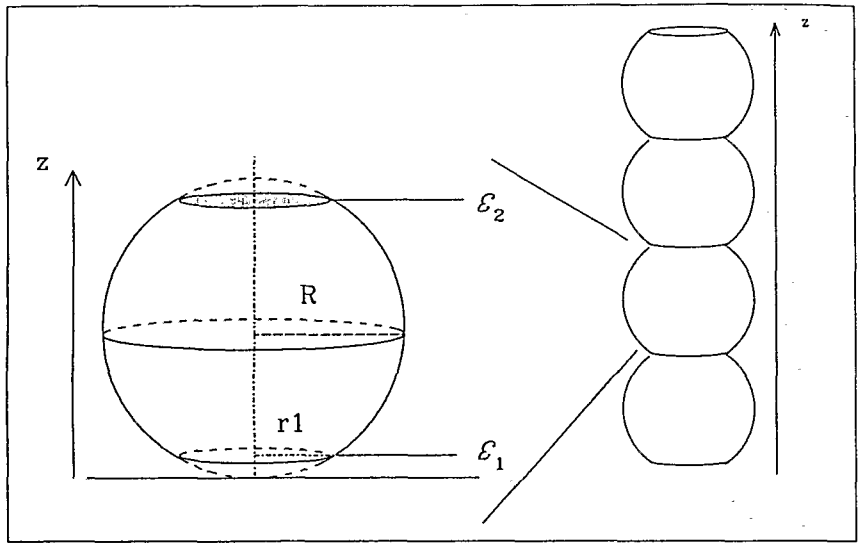

Fig. 3. Representation of the tube model constituted by a stack of hollow spherical elements. R: radius of the spherical element; r_1 access radius.

of the rock sample in which the imbibition is calculated, the calculation is extended to a stack of hollow elements (Figure 3). The evolution of the height of the meniscus versus the square root of time has been calculated for the different 'pore' shapes. The results plotted in Figure 4 show that the actual geometry of the element costituting the tube is not a relevant parameter, because identical values for R and r_1 introduced in the different pore models lead to similar imbibition kinetics. Even for the cylindrical capillary with radius R, but with a restricted entry radius of r_1, the results are equivalent. Considering the results obtained for the two normal cylindrical tubes with the radii r_1 and R, and considering the influence of the height L of the different elements (Table II), it clearly appears that the unique important parameter is the succession of necks and widenings with their respective radii: the widenings limit the capillary pressure and the necks restrain the flow rate. The slightly lower imbibition kinetics for the cylindrical tube with a restrained entry is due to the constant low capillary pressure during the whole imbibition, whereas for the other pore shapes P_c increases periodically. Porous media, such as sedimentary rocks, are formed by widenings and throats, and therefore the model composed of a stack of spherical elements (Hammecker *et al.*, 1993) has been used for this study.

In practical terms, in order to feed this calculation model, it is necessary to introduce two parameters: the radius of the pore R, and the radius of the access to the pore r_1. Their experimental determination can be performed with two different methods.

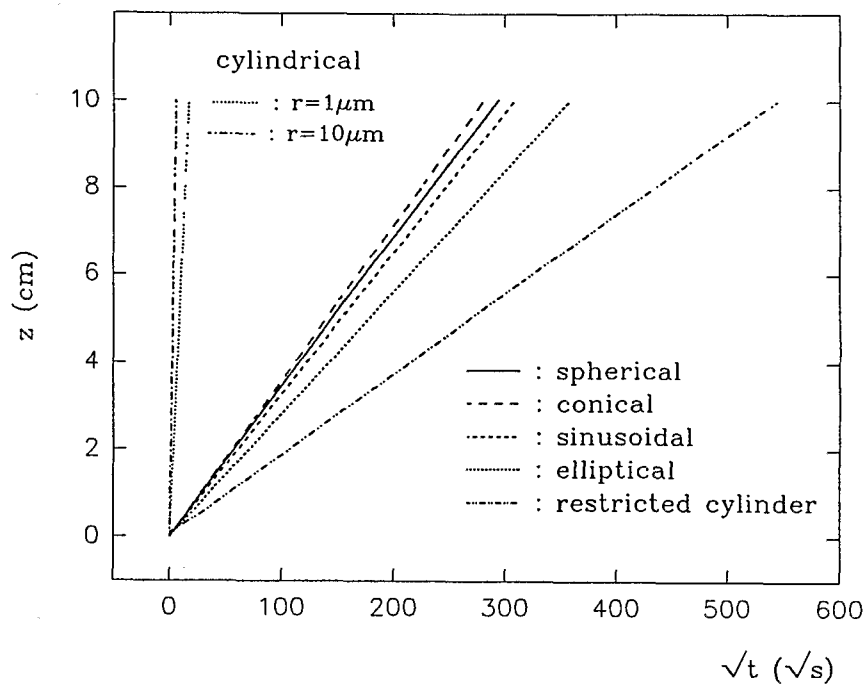

Fig. 4. Capillary imbibition calculated for the different pore models. $R = 10\,\mu$m, $r_1 = 1\,\mu$m and $L = 15\,\mu$m.

TABLE II. Calculated rate of capillary fringe migration (B) for different pore shapes and element heights (L). The height of the stack or tube which these results have been calculated is 10 cm, the maximum radius of the pore $R = 10\,\mu$m and the pore access radius $r_1 = 1\,\mu$m

	B calculated (cm/$\sqrt{\text{h}}$)			
L (μm)	5	15	150	1500
Conical	2.14	2.14	2.14	2.14
Sinusoidal	1.97	1.95	1.95	1.95
Elliptical	1.70	1.68	1.68	1.68
Spherical	2.05			
Cylindrical (r_1)	35.5			
Cylindrical (R)	110.2			
Cylindr. ($R + r_1$)	1.102			

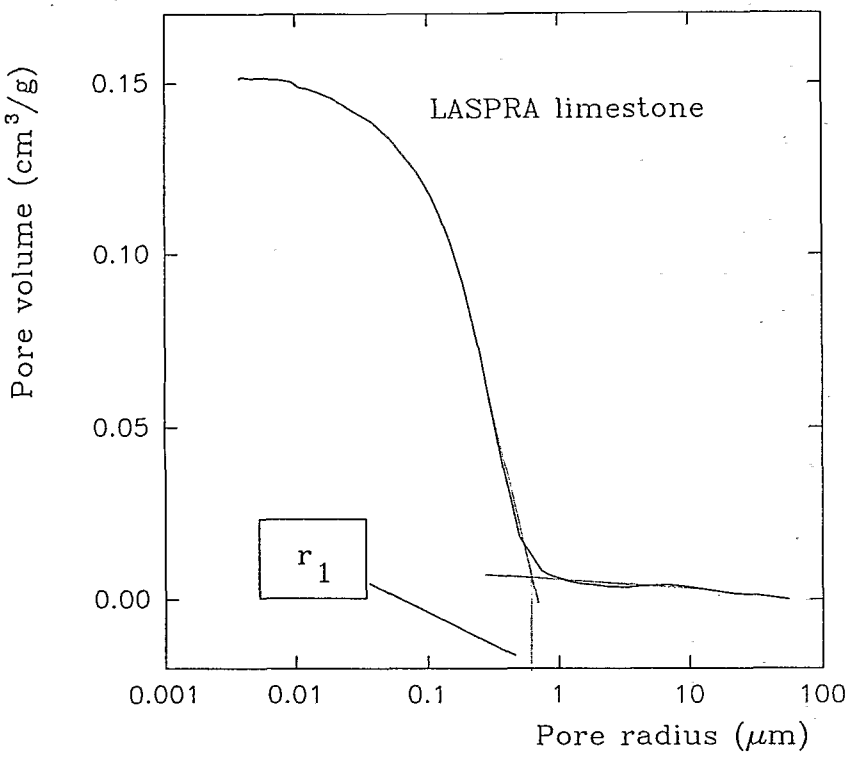

Fig. 5. Graphical method for the determination of the threshold pore access radius (r_1) on a mercury porosimetry curve.

In the direct method, R, called $R_{(\text{dir.})}$, is determined by microscopical observation of thin sections where the porosity has been filled with a coloured resin or metallic alloys (Dullien, 1981; Zinszner et Meynot, 1982). For the determination of r_1 the most usual method is mercury porosimetry. A threshold value can be determined graphically on the mercury intrusion curves (Figure 5), which represents the distribution of the necks and the pore accesses (Dullien, 1979; Chatzis and Dullien, 1981; Good and Mikhaill, 1981). The measured values for $r_{1(\text{dir.})}$ are reported in Table II.

The indirect method has been elaborated for the very fine textured rocks, when the microscopical determination of the pores radii (R) is too difficult. This method is based on the calculation of an average particle size according to the specific surface area (S) and the true density (ρ_r) of the rock. In the case of spherical particles, their average radius (R_s) is calculated as $R_s = \frac{3}{\rho_r S}$. Both pore and access radii are calculated by assuming an octahedral packing pattern of these particles. The octahedral packing has been chosen for being the most compact with the lowest

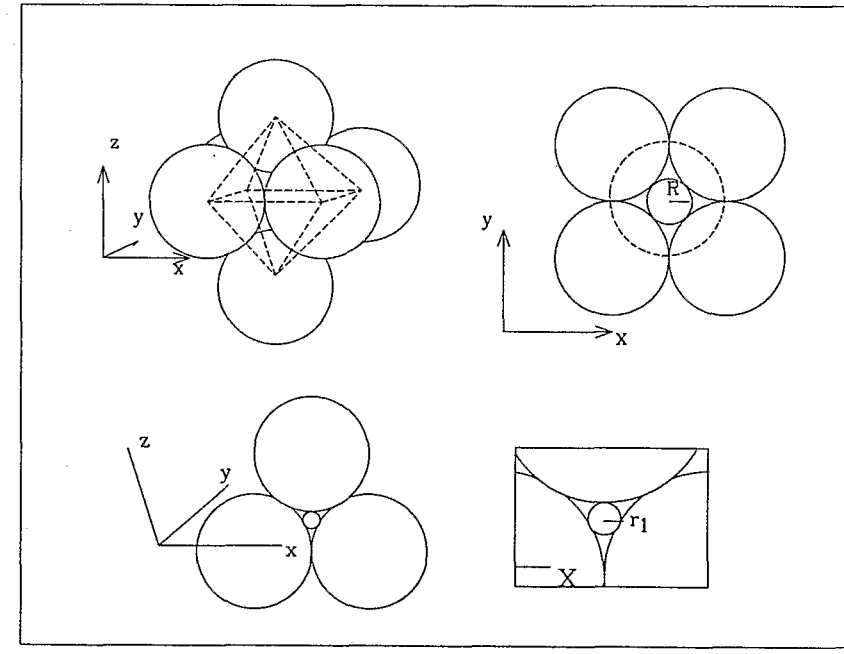

Fig. 6. Octahedral packing of isogranular spheres. R: radius of the circle fitting in the central void. r_1: radius of the circle fitting in the access to the central void.

potential energy (Graton and Fraser, 1935), and because it gives the best results in the calculation (Hammecker *et al.*, 1993). According to this particle disposition, it is possible to determine a pore radius ($R_{(\text{ind.})}$) and a pore access radius ($r_{1(\text{ind.})}$) (Figure 6). By testing the model with several specific surface areas (S) and density values (ρ_r), an empirical relation has been pointed out

$$B = \frac{9.882}{\sqrt{S\rho_r}}, \tag{7}$$

with B in $\text{cm h}^{-(1/2)}$, S in $\text{m}^2\,\text{g}^{-1}$ and ρ_r in g cm^{-3}, for the interval $0.1 < S < 50\,\text{m}^2\,\text{g}^{-1}$.

5. Application and Discussion

The model proposed by Hammecker *et al.* (1993) has been tested for the eight rocks previously described. The two methods for determination of the pore radii (R) and of the pore access radii (r_1) have been used and the results for the calculated values of B have been plotted in Figure 7. Regardless of the method used to determine the radii, there is always one of them giving a value equivalent to the experimental

TABLE III. Experimental values for specific surface area S, true density ρ_r, average pore radius R and pore access radius r_1. The calculated values are the average particle radius R_s, and the imbibition kinetics with direct ($B_{dir.}$) and indirect methods ($B_{ind.}$)

Rock type	S (m^2/g)	ρ_r (g/cm^3)	R_s (μm)	$B_{ind.}$ ($cm/\sqrt{h}$)	R (μm)	r_1 (μm)	$B_{dir.}$ ($cm/\sqrt{h}$)
Laspra	4.6	2.817	0.23	2.76	20	0.5	0.518
Lourdines	1.65	2.71	0.67	4.70	25	0.16	0.0128
Hontoria	0.8	2.668	1.40	6.76	50	1.6	1.319
Fontainebleau	0.4	2.65	2.83	9.65	45	9.5	17.61
Gueberschwihr	0.27	2.624	4.23	11.8	50	1.1	0.624
Darney	2.53	2.618	0.45	3.86	200	12	7.033
Rosheim	4.9	2.688	0.23	2.74	100	2.6	1.12
Osenbach	3.56	2.676	0.31	3.22	50	0.8	0.033
	INDIRECT METHOD				DIRECT METHOD		

value of the rate of capillary rise B. Hence this model seems to be validated, for all the different kinds of rocks. Nevertheless, it can be observed that for the slow imbibition kinetics ($B < 2\,cm\,h^{-(1/2)}$), the best agreement is obtained by using the direct method of radii determination, whereas for high B values, the indirect method gives the best results. This difference can be explained by the petrography of these rocks which depends on the mineralogy and the location of these different minerals in the rock. For all the monomineral rocks (Lourdines, Laspra, Hontoria limestones and Fontainebleau sandstone), the experimental values for B are similar to those calculated with the indirect method involving the specific surface area (S). This shows that the texture of these rocks involved in the capillary processes is perfectly described by the specific surface area. For the two micritic limestones the specific surface area is representative of the average structure of the rock, which mainly consists of an aggregation of microscopical carbonate crystallites ($\ll 5\,\mu m$). For both Hontoria limestone and Fontainebleau sandstone, the agreement between the main texture and the specific surface area is not as obvious as for the former two limestones. According to their specific surface area, the radii of the particles (R_s) are smaller than those shown by their coarse texture (Table III). Nevertheless in both cases, the texture described by the specific surface area corresponds to a microporous network present on the surface of the macropores, between the coarse grains. In Hontoria limestone it is represented by the small calcite crystals covering the macropore surfaces and the microporous intraclasts, whereas for the Fontainebleau sandstone, the surface roughness of the quartz grains, the voids between the different overgrowth and the void between the detrital grain and its overgrowth, form a continuous microporous structure, as often suggested in sandstones (Pittman, 1972; Meunier, 1992).

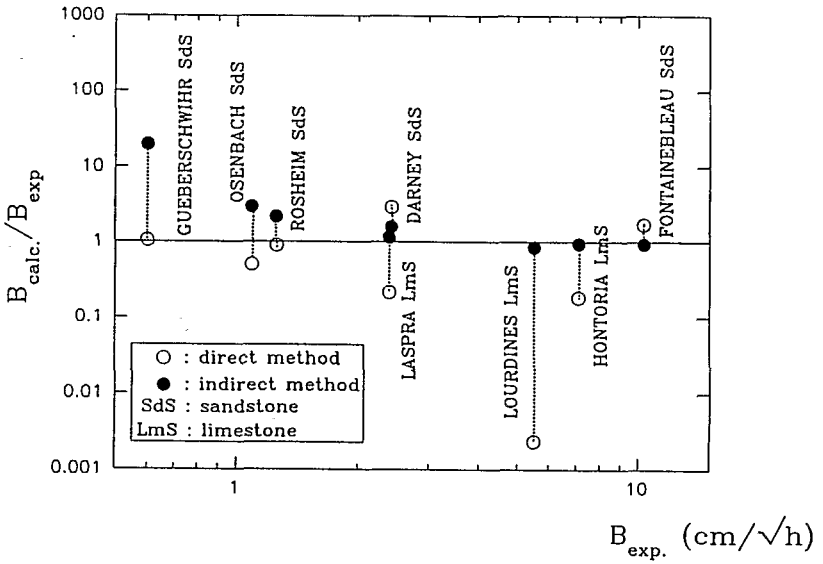

Fig. 7. Diagram representing the results for the calculated coefficient B versus the experimental one for the eight rocks.

For the other types of stones, composed of different kinds of minerals, the application of the indirect method is usually less suitable. The specific surface area of the rock is a bulk measurement which includes the specific surface area of all the different minerals. This discrepancy is especially important in the presence of clay minerals which present very high specific surface area compared to the other minerals like quartz, feldspar or muscovite. Illite, which is the most common clay mineral in these sandstones, can be considered as having a specific surface area of about $100\,m^2/g$ (van Olphen and Fripiat, 1979), whereas the specific surface area of the other minerals is much lower than $1\,m^2/g$ (e.g. $S = 0.4\,m^2/g$ for Fontainebleau sandstone, only formed by quartz). This signifies that even a low percentage of illite modifies strongly the rock's specific surface area (Figure 8). In this case, the specific surface area represents the structure of the clay minerals and not of the whole rock. Nevertheless in this case, the distribution of the clays throughout the rock determines whether the indirect method can be used or not. When the clay minerals are present as isolated clusters in the macropores, like in Rosheim and Osenbach sandstones, the pore dimensions must be determined by direct method because the kinetics of capillary transfer depends on the macroscopical pore structure. On the other hand, when they are homogeneously distributed in the rock, for example, when they form an argillaceous coating on the detrital grains (e.g. Darney sandstone), a continuous microporous network runs through the rock. Hence, the indirect method for determining the sizes of the pores must be used.

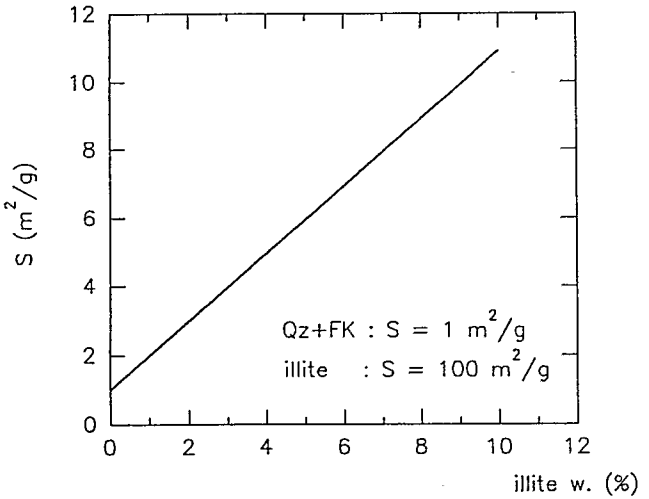

Fig. 8. Evolution of the specific surface area S of a theoretical sandstone, versus the illite content.

For Gueberschwihr sandstone, the presence of 'bare' quartz, feldspar, muscovite, and sometimes small quantities of illite, is a factor increasing the heterogeneity of the rock's surface. But the most important factor of superficial heterogeneity in this rock, is due to the fact that feldspars present both, smooth external crystalline surfaces, and very fine structures in their microporous centres, where dissolution occurs first.

Capillary processes are surface phenomena, so they depend directly on the superficial conditions of the minerals grains. When the surface properties of these grains are homogeneous in the rock, because they have the same superficial texture (Figure 9), the specific surface area is the best method for determining the kinetics of capillary imbibition.

6. Conclusions

It has been shown that regardless of the actual pore shapes, the capillary imbibition kinetics of water into sedimentary rocks, only depends on the widenings and the necks radii, through which the imbibition takes places. Therefore a numerical model involving petrographic data (Hammecker *et al.*, 1993) has been used in order to simulate the capillary imbibition kinetics.

For the eight different sedimentary rocks used in this study (limestones and sandstones), this model gives accurate results compared to the experimental ones. The data introduced in the model are two radii, R and r_1 whether measured directly on thin section and with mercury porosimetry or deduced from the specific surface area. The first method takes into account the grain size-scale texture of the

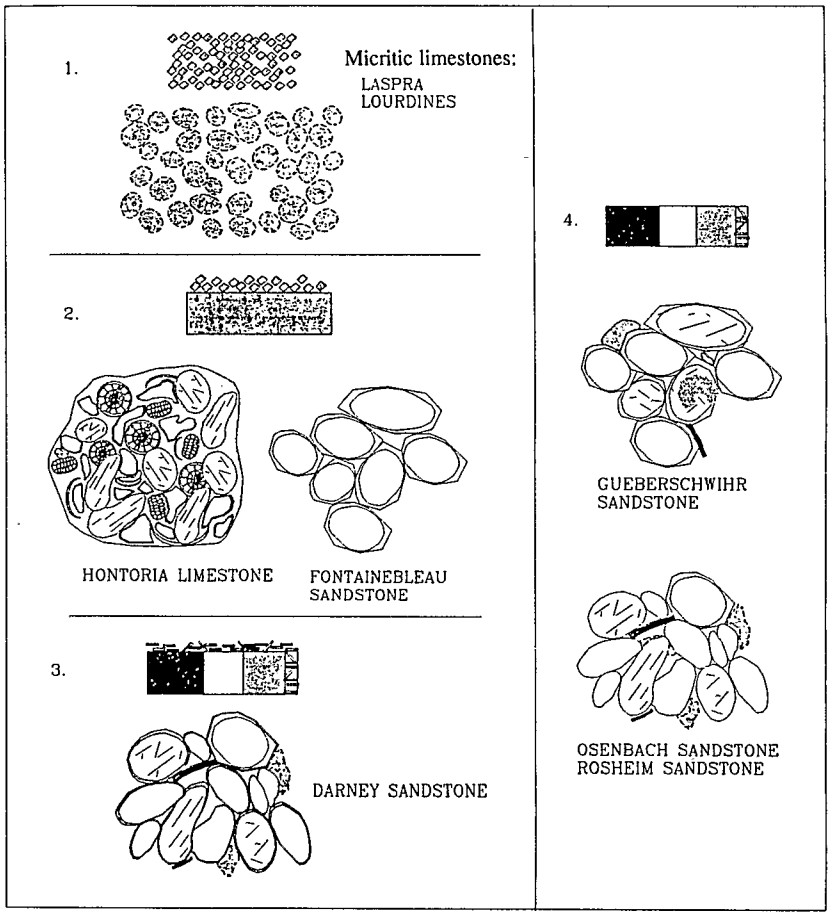

Fig. 9. Schematic representation of the structure of the rocks and their surface. 1: monomineral rocks with homogeneous texture. 2: Monomineral rocks with homogeneous surface texture. 3: Polymineral sandstone with a homogeneous surface texture. 4: Polymineral rock with heterogeneous texture.

rock, whereas the second method considers microscopical feature like the surface roughness on grains and the clay minerals texture. For both the monomineral rocks and the sandstone with illite coating, the dimensions of the pores governing the capillary transfer, are perfectly described by the specific surface area. This means that the capillary imbibition is affected not only by the presence of clay minerals, but especially by their location in the rocks. Regardless of the mineralogy and the size of the grains, the presence of an argillaceous coating leads to the homogenisation of the porous network involved in capillary processes.

In polymineral rocks, with different surface conditions, and especially with isolated clusters of clay minerals, the kinetics of capillary imbibition are determined by the 'macroscopical' porous network because of the surface heterogeneity. As capillary processes are surface phenomena, the surface homogeneity or heterogeneity of the rocks, determines the imbibition kinetics which is always higher in sandstones with an argilleous coating (e.g. Darney), than in clayey sandstones (e.g. Gueberschwihr, Rosheim and Osenbach).

Whatever the type of rock (sandstone or limestone), the presence of an homogeneous surface of the grains leads to high capillary imbibition kinetics.

References

Amoroso, G. G. and Fassina, V.: 1983, in *Stone Decay and Conservation,* Materials Science Monographs, 1, Elsevier, Amsterdam, pp. 12–42.

Chatzis, I. and Dullien, F. A. L.: 1981, Mercury porosimetry curves of sandstones, Mechanisms of mercury penetration and withdrawal, *Powder Technol.* **29**, 117–125.

Dullien, F. A. L.: 1979, *Porous Media: Fluid Transport and Pore Structure*, Academic Press, New York, pp. 291–300.

Dullien, F. A. L.: 1981, Wood's metal porosimetry and it's relation to mercury porosimetry, *Powder Technol.* **29**, 109–116.

Dullien, F. A. L., El-Sayed, M. S., and Batra, V. K.: 1977, Rate of capillary rise in porous media with non uniform pores, *J. Colloids Interface Sci.* **60**, 497–506.

Good, R. J. and Mikhail, R. S.: 1981, The contact angle in mercury porosimetry, *Powder Technol.* **29**, 53–62.

Graton, L. C. and Fraser, H. J.: 1935, Systematic packing of spheres with particular relation to porosity and permeability, *J. Geology* **43**(8), 785–909.

Hammecker. C.: 1993, Importance des transferts d'eau dans la dégradation des pierres en œuvre, Thèse Univ. Louis Pasteur, Strasbourg.

Hammecker, C., Mertz, J. D., Fischer, C., and Jeannette, D.: 1993, A geometrical model for numerical simulation of capillary imbibition in sedimentary rocks, *Transport in Porous Media* **12**, 125–141.

Jeannette, D. and Hammecker, C.: 1993, Importance des structures de porosité dans l'altération des pierres des monuments, Coll. de l'Académie des Sciences et du Cadas *"Sédimentologie et Géochimie de la Surface"* à la mém. de G. Millot, 27 et 28 Avril, pp. 307–319.

Mertz, J. D.: 1991, Structures de porosité et propriétés de transport dans les grès, *Sci. Géol. Mém.* **90**, 149 pp.

Kusakov, M. M. and Nekrasov, D. N.:1966, Capillary hysteresis in the rise of wetting liquids in single capillaries and porous bodies, in B. V. Deryagin (ed), *Research in Surface forces*, New York, pp. 193–202.

Levine, S., Lowndes, J., and Reed, P.: 1980, Two-phase fluid flow and hysteresis in a periodic capillary tube, *J. Colloid Interface Sci.* **77**, 253–263.

Lewin, S. Z. and Charola, A. E.: 1979, The physical chemistry of deteriorated brick and its impregnation techniques, in *Atti del Convegno Internazionale Il Mattone di Venezia*, Venice, October 22–23, pp.189–214.

Marmur, A.: 1989, Capillary rise and hysteresis in periodic porous media, *J. Colloid Interface Sci.* **127**, 362–372.

Meunier, J. D.: 1992, Precipitation of minerals between detrital quartz and quartz overgrowths in sandstones, *Eur. J. Mineral.* **4**, 1401–1406.

Pittman, E. D.: 1972, Diagenesis of quartz sandstones as revealed by scanning electron microscopy, *J. Sed. Petrology* **42**(3), 507–519.

Szekely, J., Neumann, A. W., and Chuang, Y. K.: 1971, The rate of capillary penetration and the applicability of the Washburn equation, *J. Colloid Interface Sci.* **35**, 273–283.

van Brakel, J.: 1975, Pore space models for transport phenomena in porous media. Review and evaluation with special emphasis on capillary transport, *Powder Technol.* **11**, 205–236.

van Olphen, H. and Fripiat, J. J.: 1979, *Data handbook for clay materials and other non metallic minerals*, Pergamon, London.

Washburn, E. W.:1921, The dynamics of capillary flow, *Phys. Rev.* **17**, 273–283.

Zinszner, B. and Meynot, C.: 1982, Visualisation des propriétés capillaires des roches réservoirs, *Rev. Inst. Franç. du Pétrole* **37**, 337–361.